

# Diazonium Ions. Topological Electron Density Analysis of Cyclopropeniumyldiazonium Dications and of Their Stability toward Dediazonation

Rainer Glaser

Departments of Chemistry, University of Missouri in Columbia, College Avenue, Columbia, Missouri 65211, and Yale University, New Haven, Connecticut 06511

Received 21 June 1989; accepted 29 November 1989

Results are presented of topological analyses of the electron density functions of cyclopropeniumyldiazonium dication, **1**, of its 2,3-diamino derivative, **2**, and of their products **3** and **4**, respectively, formed by dediazoniative ring-opening. The new CN-bonding type in **1** and **2**, recently realized synthetically in derivatives of **2**, is compared to prototypical aliphatic diazonium ions with regard to electronic structure and thermodynamic stability, factors that both are crucial for the appreciation of the mechanisms of deamination reactions of chemical and biochemical significance. Association of the dication with  $N_2$  involves density accumulation in the CN bonding region, occurs without major overall charge transfer, and leads to an electrostatically favorable quadrupolar charge distribution in the diazonium ion. The CN-bonding model recently proposed for aliphatic diazonium ions also applies to these dications. **1** is thermodynamically stable while the dediazonation of **2** is exothermic but kinetically hindered. Our best estimates for the reaction energies of the dediazoniations  $1 \rightarrow 3 + N_2$  and  $2 \rightarrow 4 + N_2$ , respectively, are 65.5 and  $-7.2$  kcal/mol, respectively. We have found that, in general, the cation is destabilized and that  $N_2$  is stabilized upon CN-bond cleavage. Cations force  $N_2$  to form diazonium ions. The remarkable difference between the stabilities of **1** and **2** is primarily due to the larger destabilization of the open dication **3** compared to **4**. Push-pull interactions between the diazo- and the overall electron-withdrawing amino-functions characterize the electronic structure of **2**. CN-Bonding and the overall electronic structure of **2** are incompatible with the usual Lewis resonance notations. Instead of dismissing the Lewis notations, it is shown that the topological description can be reconciled with the Lewis notations if the resonance forms are interpreted in a way that appropriately reflects the atom populations and first moments. Implications of the model with regard to reactivity are discussed.

## INTRODUCTION

The thermal stability of the CN linkage in aliphatic diazonium ions varies remarkably depending on the degree of unsaturation of the hydrocarbon fragment. Alkyldiazonium ions are extremely reactive intermediates that decompose readily by dediazonation.<sup>3</sup> The thermal stabilities of alkenyldiazonium salts toward loss of  $N_2$  vary greatly.<sup>4-6</sup> Alkenyldiazonium ions with heterosubstituents in the  $\beta$ -position(s) are rather stable toward loss of  $N_2$  and undergo  $C_\beta-S_N2t$ -type chemistry,<sup>4</sup> but vinyl cations<sup>7</sup> usually are spontaneously formed by dediazonation of  $\beta$ -alkyl-substituted alkenyldiazonium ions.<sup>6</sup> By analogy, ethynyldiazonium ions had been regarded as possible precursors for the generation of C-*sp*-centered carbenium ions, but solvolytic dediazoniations of phenylethyndiazonium salts were found to proceed primarily via vinyl-diazonium ions and not by  $S_N1$ -reaction.<sup>8</sup> Theoretical studies showed that the thermal cleavage of the C-*sp*-attached diazo function of the parent

ethynyldiazonium is greatly endothermic and also would involve a significant activation barrier.<sup>9-11</sup> Recently a novel type of diazonium-CN-linkage has been realized with the synthesis of various salts of 2,3-di-(dialkylamino)-cyclopropenium-1-yl-diazonium dications by Weiss, Wagner, Priesner, and Macheleid.<sup>12</sup>

Here we report the results of a theoretical study of cyclopropeniumyldiazonium dications. The focus of this article is the topological electron density analysis<sup>13</sup> of the interesting new bonding situation in the 2,3-diaminocyclopropenium-1-yl-diazonium dication, **2**. The electronic structure of **2** is characterized and compared to the parent system, cyclopropeniumyldiazonium dication, **1**. The electronic structures of the CN-linkages and their stabilities are analyzed and discussed with regard to the results of our previous studies of the prototypical methyl, vinyl, and ethynyldiazonium ions.<sup>14</sup> The main course of the thermal dediazonation of the diaminocyclopropeniumyl-diazonium dications involves a ring-opening process. The reaction energies

for these fragmentation reactions are reported for **1** and **2** and their remarkably large difference is examined.

The presented model of the bonding in these diazonium ions is based on the topological properties, on the integrated atom populations, and on the atomic first moment contributions to the molecular dipole. All of these parameters are determined from the *ab initio* electron density functions. Intrinsically there is not one model that fully describes all the richness of the electron density of a molecule. Yet, bonding models that allow for an interpretation of the complex and complete description of the molecule by its electron density distribution (via its wave function) are basic to a chemist's reflections in the analyses of chemical processes as well as to his predictive ability in judging new synthetic strategies. Our model recovers the essential features of the electron density distributions and it is capable to explain the chemistry of these systems, and in these regards the model presented is superior to the usual model based on Lewis resonance structures. It is shown that both models can be reconciled if the Lewis structures are interpreted as notations from which the directions of internal polarizations can be deduced.

## RESULTS AND DISCUSSION

### Structures and Stability

Gradient optimizations<sup>15,16</sup> were performed under the constraints of the symmetry point groups specified. The Hessian matrix and harmonic vibrational frequencies were calculated analytically to characterize stationary structures as minima, transition state structures, or second-order saddle points, and to obtain vibrational zero-point energies (VZPEs). Zero-point energy corrections to relative energies and reaction energies were scaled (factor 0.9) since they are generally overestimated at this computational level.<sup>17</sup> Optimizations and characterization of stationary structures were carried out with restricted Hartree-Fock (RHF) wave functions with the 3-21G basis set.<sup>18</sup> The analytically calculated forces were then used for subsequent structural refinement at the RHF/6-31G\* level.<sup>19</sup> Energies were calculated with the RHF/6-31G\* geometries at levels of Møller-Plesset perturbation theory<sup>20</sup> up to MP4[SDQ]/6-31G\* in the frozen core approximation to account, in part, for electron correlation.

Total energies of the equilibrium and saddle point structures of **1**, the equilibrium structure of **2**, and of their dediazonation products **3** and **4** are given in Table I, and the thermodynamic sta-

bilities of the diazonium dications are summarized in Table II. Structural parameters are collected in Table III and Tables containing the harmonic vibrational frequencies are available as Supplemental Material.

### Cyclopropenyldiazonium Dication

Of the  $C_{2v}$ -symmetric structures **1a**–**1c** (Fig. 1) only **1a** is a minimum. The transition vector ( $i555.4 \text{ cm}^{-1} b_1$ ) identifies **1b** as the transition state structure for automerization of **1a**, and the planar structure **1c** corresponds to a second-order saddle point ( $i548.4 \text{ cm}^{-1} b_2, i79.9 \text{ cm}^{-1} a_2$ ) on the RHF/3-21G potential energy hypersurface. **1c** remains roughly 2 kcal/mol less stable than **1b** at all levels (Table II).

Polarization functions have a significant effect on bond lengths (Table III). The structures optimal at RHF/6-31G\* are discussed. The unique CC-bond in **1a** (1.389 Å) is 0.053 Å longer than the other CC-bonds, and this bond length greatly depends on whether the  $N_2$ -unit is rotated in or out of the plane of the three-membered ring. The C2C3-bond in **1b** is 0.033 Å longer than in **1a**, while it is practically unaltered in the planar spiro-system **1c**. The CC-bonds to the C1-atom are shortened in going from **1a** to the edge-on coordinated structures.

### 2,3-Diaminocyclopropenyldiazonium Dication

Only the planar structure **2** has been considered for this system. The analytical computation of the Hessian matrix at the RHF/3-21G level shows **2** to be a minimum. The geometry optimal at RHF/6-31G\* is illustrated in Figure 2. The  $NH_2$ -substituents *lengthen* both the C1C2-bond (by 0.020 Å) and the unique C2C3-bond (by 0.056 Å) while the CN(N)-distance is shorter (by 0.019) in **2** compared to **1a**. The *ab initio* structure is more "compact" compared to the MNDO structure;<sup>12</sup> except for the CN-bond, all bonds are (significantly) shorter.

### Thermodynamic Stability toward Dediazoniative Ring-Opening

The main course of thermal dediazonation of the cyclic diazonium ions involves a ring-opening process and products of Baltz-Schiemann-type reactions also were identified.<sup>12</sup> Both of these processes presumably involve a more or less dication of cyclopropylidene<sup>26</sup> that reacts with a nucleophile either before or after ring-opening. Since an adequate theoretical treatment of the cyclopropylidene dication is likely to require

Table I. Symmetry properties, character, vibrational zero-point energies, and energy

Molecule <sup>a</sup>	Number	PG <sup>b</sup>	DOF <sup>c</sup>	CSS <sup>d</sup>	VZPE <sup>e</sup>	A
Cyclopropeniumyldiazonium Dication						
end-on	1a	C <sub>2v</sub>	6	M	27.21	221.458
edge-on, out of plane	1b	C <sub>2v</sub>	6	TS	24.00	221.325
edge-on, in plane	1c	C <sub>2v</sub>	6	SOSP	23.93	221.322
2,3-Diaminocyclopropenium-1-yl-diazonium Dication						
end-on	2	C <sub>2v</sub>	10	M	50.14	331.077
Didehydrided Allene	3	D <sub>2h</sub>	2	M	19.23 <sup>f</sup>	113.054
Didehydrided Diaminoallene	4	D <sub>2d</sub>	4	M	43.25	222.798

<sup>a</sup>Compare Figures 1 and 2.

<sup>b</sup>Symmetry point group.

<sup>c</sup>Degrees of freedom.

<sup>d</sup>Character of the stationary structure: M = minimum (Number of Imaginary frequency = 0), TS = transition state (Number of Imaginary frequency = 1), SOSP = second order saddle point structure (NIMAG = 2).

<sup>e</sup>Vibrational zero-point energies (RHF/3-21G) are scaled by a factor of 0.9.

<sup>f</sup>Scaled VZPE of 3 at RHF/6-31G\* 19.00 kcal/mol.

<sup>g</sup>Energies ( $-E$ ) in atomic units. RHF energies are reported for the levels RHF/3-21G. MPx energies are at MPx(fc)/6-31G\*/RHF/6-31G\*.

es of stationary structures.

	RHF		MP2	MP3	MP4	
	A/B	B			DQ	SDQ
3	222.75749	222.75854	223.39647	223.40577	223.41051	223.41865
2	222.65725	222.66270	223.30278	223.31309	223.31552	223.32416
5	222.65356	222.65980	223.29920	223.31016	223.31239	223.32082
7	332.95650	332.95769	333.94133	333.95164	333.95659	333.96902
7	113.69855	113.69863	114.04521	114.04184	114.04143	114.05383
9	224.02156	224.02156	224.69362	224.71112	224.71138	224.72167

encies = 0), TS = transition state structure (NIMAG = 1), and SOSP = second-

(A), RHF/6-31G\*\*//RHF/3-21G (A/B), and RHF/6-31G\* (B). Møller-Plesset cal-

**Table II.** Thermodynamic stabilities.<sup>a-c</sup>

Molecule	RHF			MP2	MP3	MP4	
	A	A/B	B			DQ	SDQ
1a	60.0	67.6	68.2	60.1	69.8	70.5	65.5
1b	-20.3	7.9	11.2	4.5	14.9	14.2	9.4
1c	-21.9	5.6	9.5	2.4	13.1	12.3	7.3
2	-17.5	-9.1	-8.4	-3.8	-6.5	-6.1	-7.2

<sup>a</sup>Energies for the dediazonation reactions  $1 \rightarrow 3 + N_2$  and  $2 \rightarrow 4 + N_2$  in kcal/mol. Values include scaled vibrational zero-point energies (cf. Table I).

<sup>b</sup>RHF reaction energies at the levels 3-21G (A), 6-31G\*/3-21G (A/B) and 6-31G\* (B).

<sup>c</sup>MPx(fc)/6-31G\*/RHF/6-31G\*.

**Table III.** Structures of cyclopropenyldiazonium dications and of 2,3-diamino-cyclopropenium-1-yl-diazonium dication.<sup>a-d</sup>

	1a		1b		1c		2	
	3-21G	6-31G*	3-21G	6-31G*	3-21G	6-31G*	3-21G	6-31G*
N1—N2	1.082	1.078	1.114	1.105	1.114	1.108	1.084	1.078
C1—N1	1.367	1.394	1.923	1.760	1.943	1.750	1.350	1.375
C1—C2	1.350	1.336	1.326	1.321	1.328	1.330	1.369	1.356
C2—C3	1.397	1.389	1.455	1.422	1.445	1.397	1.461	
C2—E <sup>b</sup>	1.073	1.082	1.077	1.084	1.076	1.084	1.271	1.277
N—H1							1.012	1.006
N—H2							1.011	1.006
C2—C1—C2	62.3	62.6	66.6	65.1	65.9	63.4	64.5	64.4
N—C1—N			37.4	40.7	37.0	41.0		
E—C2—C1 <sup>b</sup>	151.3	151.6	156.0	155.0	155.4	152.6	153.2	153.3
H1—N3—C2							122.3	121.7
H2—N3—C2							122.2	121.6

<sup>a</sup>In Å and degrees. See Figures 1 and 2.

<sup>b</sup>E = H for 1 and E = N for 2.

<sup>c</sup>Structure(s) of didehydrided allene ( $D_{2h}$ ) at 6-31G\* (and 3-21G): HC = 1.098 (1.094), CC = 1.253 (1.249).

<sup>d</sup>Structure(s) of didehydrided diaminoallene ( $D_{2d}$ ) at 6-31G\* (and 3-21G): HN = 1.019 (1.028), HNC = 121.6 (122.5), NC = 1.237 (1.235), CC = 1.261 (1.253).

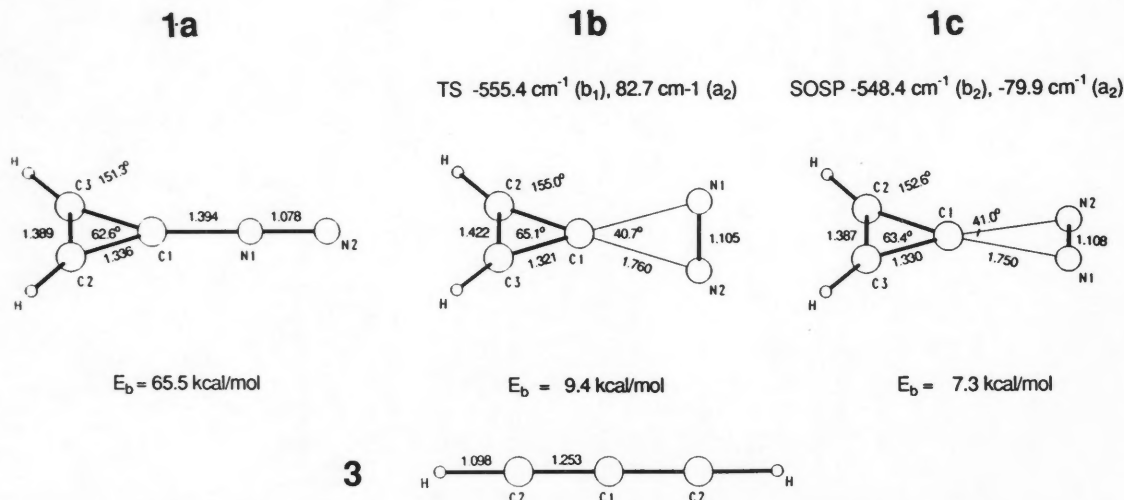


**Figure 1.** Cyclopropenyldiazonium dication 1. Molecular-model-type drawings of stationary structures of 1 and of didehydrided allene 3 as determined at the RHF/6-31G\* level. Energies  $E_b$  (in kcal/mol) for reactions  $1 \rightarrow 3 + N_2$  are those determined at the MP4[SDQ]/6-31G\*/RHF/6-31G\* level and they include vibrational zero-point energy corrections. Frequencies of imaginary vibrational modes are given to characterize higher-order stationary structures.

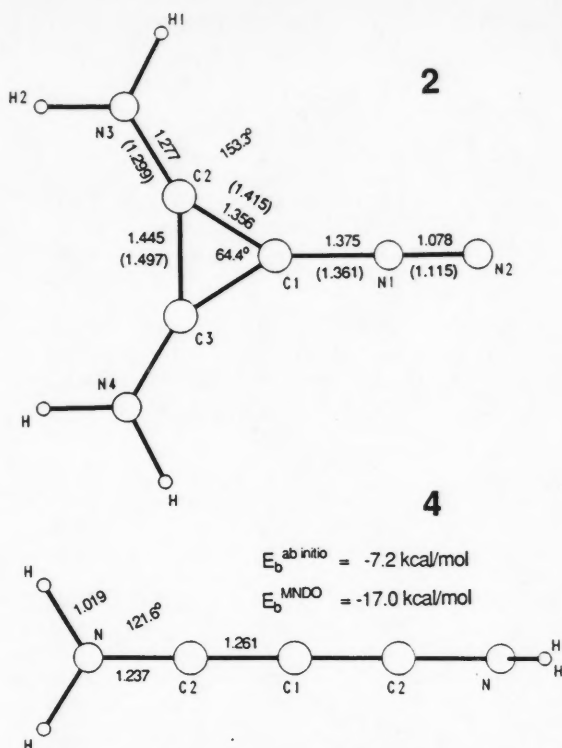


**Figure 2.** 2,3-Diamino-Cyclopropenium-1-yl-diazonium dication **2**. Molecular-model-type drawings of the equilibrium structures of **2** and of didehydrided 1,3-diaminoallene **4**, the product of dediazonation with concomitant ring opening, as calculated at the RHF/6-31G\* level. The energy  $E_b$  (in kcal/mol) for the reaction  $2 \rightarrow 4 + N_2$  is that calculated at the MP4 [SDQ]/6-31G\*\*/RHF/6-31G\* level and includes vibrational zero-point energy corrections.

large-scale CI-calculations, here we consider only the dediazonation reactions leading to the ring-opened dications, **3** ( $D_{\infty h}$ ) and **4** ( $D_{2d}$ ). These dications formally arise from twofold hydride abstraction from allene and 1,3-diaminoallene, respectively.

Energies for the reactions  $1 \rightarrow 3 + N_2$  and  $2 \rightarrow 4 + N_2$  are summarized in Table II. Binding energies derived at the RHF/3-21G level are greatly in error, but binding energies calculated at RHF/6-31G\* agree well with the respective values obtained at the MP3 level and the higher levels of perturbation theory.<sup>27</sup> In our previous study of diazonium ions reasonable agreement was obtained between theoretical and experimental binding energies at the MP3/6-31G\*\*/RHF/6-31G\* or higher levels. The reaction energies reported here are likely to be within 5–8 kcal/mol of the true gas-phase reaction energies.<sup>14</sup> The dediazonation of **2** with concomitant ring-opening is exothermic by 7.2 kcal/mol at the MP4[SDQ]/6-31G\*\*/RHF/6-31G\* level and including vibrational zero-point energy cor-

rections. MNDO correctly predicts this reaction to be exothermic but overestimates the reaction energy (17 kcal/mol).<sup>12</sup> The parent system **1a** is not only kinetically but also thermodynamically stable toward this mode of dediazonation; at the highest level the dediazonation of **1a** is endothermic by 65.5 kcal/mol. Thus, the amino-substituted system **2** is about 72.7 kcal/mol less stable toward dediazonation. The origin of this large difference will be analyzed below.

### Electron Density Analysis

The topological characterization of the molecular electron densities is based on the properties of the gradient vector field of the electron density,  $\nabla\rho(\mathbf{r})$ . Excellent reviews of the method are available,<sup>13</sup> and reference to relevant primary literature is made in Tables IV and VI. The electron density analyses were carried out at the RHF/6-31G\*\*/RHF/6-31G\* level. Wave functions were transformed with the program Psichk<sup>21</sup> into a format suitable for the electron density analysis programs. Topological properties were determined with the programs Extreme<sup>22</sup> and Alpha,<sup>23</sup> and the program Proaims<sup>24</sup> was used to determine fragment populations and stabilities by density integration techniques.<sup>25</sup>

Table IV summarizes pertinent results of the topological analysis. The locations of critical points in  $\rho(\mathbf{r})$  are given by the distances  $r_A$  and  $r_B$  between the critical point and the positions of the atoms *A* and *B*, respectively, and the parameter *F* as defined in Table IV. Critical points in  $\rho(\mathbf{r})$  are characterized by the magnitude of the electron density  $\rho_b$ , the eigenvalues  $\lambda_i$  of the Hessian matrix of  $\rho(\mathbf{r})$ , that is, the principal curvatures of  $\rho(\mathbf{r})$  at the critical point, and the Laplacian  $\nabla^2\rho(\mathbf{r}) = \sum\lambda_i$ . Bond path angles of **1a** and **2** are listed in Table V. Subspaces within  $\rho(\mathbf{r})$ , so-called basins, are defined as regions in Cartesian space bounded by a zero-flux surface of the gradient vector field of  $\rho(\mathbf{r})$ , that is, a surface for which  $\nabla\rho(\mathbf{r}) \cdot \mathbf{n}(\mathbf{r}) = 0$  at all points. Important properties of such basins are summarized in Table VI. The values reported include populations of atoms and atom groups, *N*, the contributions to the integrated populations associated with  $\pi$ -orbitals,  $N_\pi$ , and energies of atoms and atom groups, *T* and *T'*.

### Nature of the CN-Bonding

**Topological Properties.** Usually exocyclic C-*sp*-orbitals are discussed for **1a** and **2** based on the  $J(^{13}\text{C-H})$  coupling constants of related systems.<sup>29</sup> Such practice implies a description of the  $\sigma$ -framework of the three-membered ring with bent bonds formed between C-*sp*<sup>3</sup>-hybrid or-

**Table IV.** Topological properties of cyclopropeniumdiazonium dications, 2,3-diamino-cyclopropenium-1-yl-diazonium dication, and of didehydrided allene and diaminoallene.<sup>a</sup>

Bond	$r_A^b$	$r_B$	$F^c$	$\rho_b^d$	$\nabla^2(\rho)^e$	$\lambda_1^f$	$\lambda_2$	$\lambda_3$	$\varepsilon^g$
Cyclopropeniumdiazonium Dication, 1a									
C1 N1	0.436	0.957	0.313	0.259	0.074	-0.598	-0.437	1.109	0.367
N1 N2	0.596	0.482	0.553	0.674	-2.592	-1.561	-1.518	0.486	0.028
C1 C2	0.737	0.611	0.547	0.332	-0.920	-0.576	-0.547	0.203	0.052
C1 C2 <sup>h</sup>	0.762	0.791	0.491	0.260	0.378	-0.307	0.333	0.352	
C3 C2	0.698	0.698	0.500	0.318	-0.802	-0.590	-0.508	0.295	0.162
C2 H	0.782	0.300	0.727	0.284	-1.355	-0.915	-0.903	0.462	0.014
Cyclopropeniumdiazonium Dication, 1b									
C1 N	0.750	1.074	0.411	0.133	-0.020	-0.226	-0.093	0.299	1.433
N N	0.553	0.553	0.500	0.688	-2.670	-1.903	-1.581	0.814	0.203
C1 C2	0.715	0.620	0.535	0.343	-0.976	-0.598	-0.587	0.208	0.022
C1 C2 <sup>h</sup>	0.749	0.799	0.484	0.261	0.344	-0.314	0.296	0.362	
C2 C2	0.712	0.712	0.500	0.301	-0.647	-0.542	-0.414	0.309	0.311
C2 H	0.789	0.295	0.728	0.282	-1.362	-0.919	-0.908	0.465	0.013
Cyclopropeniumdiazonium Dication, 1c									
C1 N	0.747	1.068	0.412	0.137	-0.029	-0.247	-0.081	0.299	2.045
N N	0.554	0.554	0.500	0.685	-2.653	-1.898	-1.582	0.827	0.200
C1 C2	0.740	0.601	0.552	0.332	-0.911	-0.564	-0.531	0.183	0.061
C1 C2 <sup>h</sup>	0.745	0.798	0.483	0.263	0.357	-0.299	0.323	0.333	
C3 C2	0.701	0.701	0.500	0.314	-0.745	-0.566	-0.473	0.295	0.196
C2 H	0.787	0.297	0.726	0.282	-1.357	-0.915	-0.905	0.464	0.011
2,3-Diaminocyclopropenium-1-yl-diazonium Dication, 2									
C1 N1	0.428	0.947	0.311	0.258	0.441	-0.489	-0.405	1.345	0.229
N1 N2	0.606	0.473	0.562	0.673	-2.605	-1.547	-1.504	0.446	0.029
C1 C2	0.686	0.687	0.500	0.320	-0.840	-0.588	-0.517	0.266	0.178
C1 C2 <sup>h</sup>	0.784	0.889	0.492	0.231	0.417	-0.273	0.325	0.365	
C2 C3	0.728	0.728	0.500	0.284	-0.672	-0.539	-0.451	0.319	0.196
C2 N3	0.430	0.847	0.337	0.385	-0.885	-0.946	-0.839	0.901	0.128
N3 H1	0.791	0.215	0.786	0.328	-1.745	-1.407	-1.371	1.033	0.027
N3 H2	0.790	0.215	0.786	0.329	-1.751	-1.414	-1.376	1.039	0.027
Didehydrided Allene, 3									
C1 C2	0.433	0.820	0.346	0.389	-0.599	-0.684	-0.684	0.768	0.000
C2 H	0.843	0.255	0.768	0.271	-1.405	-0.976	-0.976	0.546	0.000
Didehydrided 1,3-Diaminoallene, 4									
C1 C2	0.445	0.816	0.353	0.372	-0.698	-0.741	-0.489	0.531	0.516
C2 N	0.416	0.821	0.338	0.415	-0.695	-1.125	-0.895	1.325	0.257
N H	0.810	0.209	0.795	0.312	-1.669	-1.375	-1.354	1.060	0.015
Nitrogen									
N N	0.539	0.539	0.500	0.711	-2.759	-1.699	-1.699	0.638	0.000

<sup>a</sup>At RHF/6-31G\*. See Figures 1-4.<sup>b</sup>Distance  $r_A$  ( $r_B$ ) of atom A (B) from the critical point in Å.<sup>c</sup>The distance of the critical points from atom A is given by the fraction F of the bond length  $d(AB)$ ;  $F := r_A/(r_A + r_B)$ .<sup>d</sup>Density at the critical point  $\rho^b$  (in e a.u.<sup>-3</sup>).<sup>e</sup>Laplacian  $\nabla^2(\rho)$  at the critical point (in e a.u.<sup>-5</sup>); cf. references 28d and 28f.<sup>f</sup>Eigenvalues  $\lambda_i$  of the Hessian matrix A of  $\rho(r)$  at the critical point (in e a.u.<sup>-5</sup>), see references 28a-c.<sup>g</sup>Bond ellipticity  $\varepsilon$ , defined as  $\varepsilon = \lambda_n/\lambda_m - 1$ , where  $\lambda_n < \lambda_m$  and  $\lambda_i < 0$  ( $i = n, m$ ); cf. References 28d and 28e.<sup>h</sup>Position of a (3, +1) ring critical point.

bitals.<sup>30</sup> In the topological method the directionality of the bonding can be described precisely by the molecular graph of the (observable) total electron density distribution and without consideration of (unobservable) atomic (hybrid) orbitals. The directions in which electron density is locally concentrated in the vicinity of an atom are given by the tangents to the bond paths that originate at that atom. The representations of the gradient vector field,  $\nabla\rho(\mathbf{r})$ , and of the molecular

graphs of **1a** and **2**, illustrated in Figures 3 and 4, respectively, both show bond path angles C2—C1—C3 that are about 102° (Table V). This angle is about 7° smaller than the typical angle between  $sp^3$ -hybrid orbitals and it would suggest that the CC bonds between the ring atoms involve orbitals with a higher  $p$ -character than implied by  $sp^3$ -hybridization and that the C1-orbital used for the exocyclic CN bond has a larger  $s$ -character than implied by  $sp$ -hybridization. It is stressed,

Table V. Comparison between geometric and bond path angles.<sup>a</sup>

Defined by A B C	Geometric	Bond path	$r(B-A)$	$r(B-C)$
Cyclopropenyldiazonium Dication, <b>1a</b>				
C2—C1—C3	62.64	102.59	19.98	19.98
C1—C2—C3	58.68	79.31	11.00	9.63
H6—C2—C1	151.60	140.17	0.43	11.00
2,3-Diaminocyclopropenium-1-yl-diazonium Dication, <b>2</b>				
C2—C1—C3	64.40	102.01	18.81	18.81
C1—C2—C3	57.80	84.74	14.35	12.58
C1—C2—N3	153.34	139.18	14.35	0.19
H1—N3—C2	121.73	119.83	1.75	0.15
H2—N3—C2	121.58	119.95	1.78	0.15

<sup>a</sup>In the last two columns the angles are listed that are enclosed by the internuclear axis, the vector indicated, and the corresponding bond path.

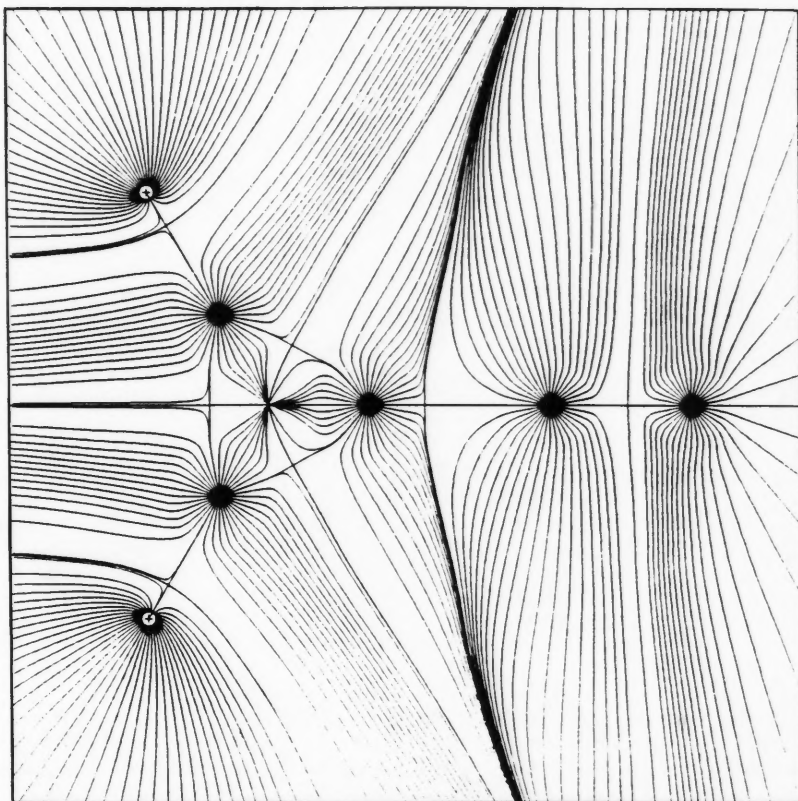


Figure 3. Graphical representations of the gradient vector field of the electron density,  $\nabla\rho(r)$ , and of the molecular graph of cyclopropenyldiazonium dication 1a. The gradient paths asymptotically approach the cross-sections of the zero-flux surfaces of  $\nabla\rho(r)$ . These cross-sections intersect with the bond paths at bond critical points.

however, that such an *interpretation* of the molecular graph in terms of hybridization cannot be rigorous. For example, the molecular graphs also show that the C1—C2—C3 (and C1—C3—C2) bond path angles are significantly smaller than 90° (Table V) and they obviously cannot be interpreted within the framework of hybridization.

The smaller angle between the CC bond paths originating at C2 (or C3) compared to the larger angle between the C1—C2 and C1—C3 bond paths indicates that the ring strain of these three-membered rings originates primarily from the electron density distributions within the basins of the C-atoms in positions 2 and 3.<sup>31</sup>

**Table VI.** Integrated atom properties of cyclopropeniumdiazonium dications, 2,3-di-aminocyclopropeniumyl-1-diazonium dication, and of didehydrided allene and 1,3-diaminoallene.<sup>a</sup>

Atom <sup>b</sup>	N <sub>π</sub> <sup>c,d</sup>	N <sup>d</sup>	L <sup>e</sup>	T <sup>f</sup>	T' <sup>g</sup>
<b>Cyclopropeniumdiazonium Dication, 1a</b>					
C1	0.891	5.624	0.00009	37.59095	37.67314
N1	1.341	7.589	-0.00021	54.90451	55.02456
N2	0.707	6.188	0.00001	53.64903	53.76633
C2	0.527	5.703	0.00003	37.63932	37.72162
H	0.003	0.596	0.00006	0.42470	0.42563
Σ	4.000	32.000			222.75853
N <sub>2</sub>	2.049	13.777			108.79089
CH	0.530	6.300			38.14725
<b>Cyclopropeniumdiazonium Dication, 1b</b>					
C1		5.895	-0.00890	37.73158	37.80160
C2		5.715	0.00003	37.64215	37.71200
H		0.577	0.00006	0.41458	0.41535
N <sub>2</sub> <sup>i</sup>		13.522			108.60641
CH		6.292			38.12735
C <sub>3</sub> H <sub>2</sub>		18.478			114.05629
<b>2,3-Diaminocyclopropenium-1-yl-diazonium Dication, 2</b>					
C1	1.140	5.558	0.00005	37.51121	37.59426
N1	1.337	7.616	-0.00028	54.94402	55.06567
N2	0.820	6.267	-0.00004	53.69883	53.81771
C2	0.616	4.954	0.00000	37.18305	37.26537
N3	1.720	8.455	0.00173	55.13528	55.25735
H1	0.008	0.436	0.00004	0.35850	0.35929
H2	0.008	0.435	0.00005	0.35876	0.35955
Σ	8.000	48.000			332.96076
N <sub>2</sub>	2.157	13.883			108.88338
NH <sub>2</sub>	1.736	9.325			55.97619
C <sub>3</sub>	2.371	15.467			112.12499
<b>Didehydrided allene, 3</b>					
C2	0.590	6.180	0.00807	37.87194	37.93597
C1	0.817	4.770	0.00000	37.08086	37.14356
H	0.001	0.441	0.00006	0.33915	0.33972
Σ	2.000	18.013			113.68494
CH	0.591	6.621			38.27569
<b>Didehydrided diaminoallene, 4</b>					
C2		5.320	0.00000	37.41685	37.48599
C1		4.846	-0.00003	37.06942	37.13792
N		8.481	0.00124	55.20093	55.30294
H		0.389	0.00005	0.32640	0.32700
Σ		34.000			224.02379
NH <sub>2</sub>		9.258			55.95694

<sup>a</sup>At RHF/6-31G\*/RHF/6-31G\*.<sup>b</sup>See Figures 4 and 5.<sup>c</sup>N<sub>π</sub> represents the contribution to N due to the π-symmetric valence-MOs.<sup>d</sup>Atomic populations N and N<sub>π</sub> in electrons.<sup>e</sup>The L-values are the volume integrals of L(r) = -0.25 · ∇<sup>2</sup>ρ(r) over the atomic basins, in atomic units; cf. reference 25.<sup>f</sup>Integrated atomic kinetic energy T in atomic units.<sup>g</sup>Integrated atomic kinetic energy corrected for the virial defect of the wavefunction, T', where T' = T · [-(V/T) - 1]. The virial ratios -V/T were: 1a 2.00218646; 1b 2.00185567; 2 2.00221396; 3 2.00169085; 4 2.00184799.<sup>h</sup>Differences between the sum T'' of the integrated kinetic energies T' of the atoms and the total energy of the molecule (-E<sub>mol</sub> = T<sub>mol</sub>), T'' + E in atomic units: 1a -0.00002; 2 +0.00307; 3 -0.00369; 4 +0.00223.<sup>i</sup>By difference.

Figures 3 and 4 show in a compelling way that the zero-flux surfaces that partition the CN- and the NN-bonding regions are shifted away from N<sub>α</sub>. The CN-bond critical points are close to C1 (F<sub>CN</sub>(1a) = 0.313, F<sub>CN</sub>(2) = 0.311) and the NN-bond critical points are shifted toward the termi-

nal N<sub>β</sub> (F<sub>NIN2</sub>(1a) = 0.553, (F<sub>NIN2</sub>(2) = 0.562). The direction of the shifts of the NN-bond critical points and the accompanying small decreases (6%) of the ρ<sub>b</sub> values compared to free N<sub>2</sub> (0.711) indicate an internal N<sub>2</sub>-polarization in the fashion N<sub>α</sub><sup>δ-</sup>N<sub>β</sub><sup>δ+</sup>. The curvatures λ<sub>1</sub> and λ<sub>2</sub> at the NN

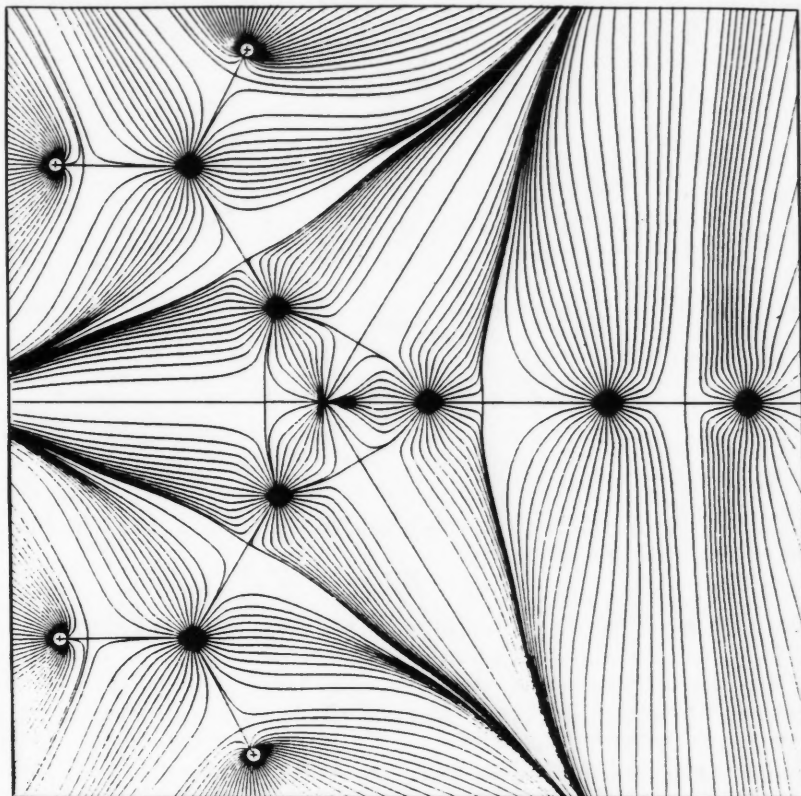


Figure 4. Graphical representations of the gradient vector field of the electron density,  $\nabla\rho(\mathbf{r})$ , and of the molecular graph of 2,3-diamino-cyclopropenium-1-yl-diazonium dication **2**. Compare legend to Figure 3.

bond critical points reflect the fall-off of  $\rho(\mathbf{r})$  with the distance from the internuclear axis. For **1a** and **2** the values of  $\lambda_1$  and  $\lambda_2$  are less negative than in free  $\text{N}_2$ ; the polarization of the  $\text{N}_2$ -groups is accompanied by a radial expansion of the electron density in the NN bonding region. Thus, **1a** and **2** show all of the typical topological features of the acyclic diazonium monocations.<sup>14</sup>

Cremer and Kraka showed that three-membered rings possess relatively high electron density in the ring plane.<sup>31</sup> This topological feature was named *surface delocalization* and considered to arise from  $\sigma$ -aromaticity. As with their systems we find that the electron densities at the ring critical points in **1a** and **2** are in excess of 70% of the electron density values found at the CC bond critical points (Table IV), but with regard to the significant differences (vide infra) in the populations of C1 and C2, particularly in **2**, we are reluctant to deduce any conclusions regarding  $\sigma$ -aromaticity from this topological result.

**Populations Analysis.** In Figure 5 atom and fragment charges are given that result from the integrated populations (Table VI). The overall

$\text{N}_2$ -charges are more positive in **1a** and **2** compared to the aliphatic diazonium ions but, more importantly, *the positive charge of the diazo-functions remains remarkably small even in these dications*. Charges of only +0.22 (**1a**) and +0.12 (**2**), respectively, are indicated by the  $\text{N}_2$ -populations. The main consequence of CN-bonding on the electronic structure of  $\text{N}_2$  is not charge transfer toward the positively charged hydrocarbon fragment but strong internal polarization. Mulliken populations indicate  $\text{N}_2$ -charges that are too large, primarily because of underestimation of the  $\text{N}_\alpha$ -population. For example, the MNDO Mulliken population<sup>12</sup> of  $\text{N}_\alpha$  in **2** is 6.83 whereas the integrated population is 7.62. In the Mulliken scheme overlap populations are equally divided between the bonded atoms and the method therefore intrinsically does not account sufficiently for the substantial CN-bond polarities (vide supra), whereas the integrated populations do reflect this feature.<sup>32</sup>

**CN Bonding Model.** As with the prototypical diazonium cations, CN bonding in the diazonium dications can be described with a bonding model that involves  $\sigma$ -donation from  $\text{N}_2$  to the positively

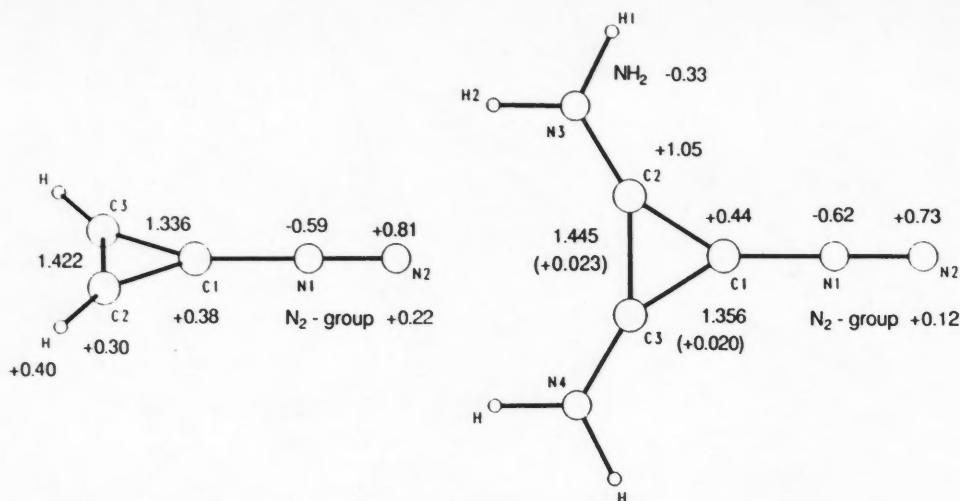


Figure 5. Populations derived by electron density integration show that the  $\text{NH}_2$ -substituents are overall electron-withdrawing.

charged hydrocarbon fragment and simultaneous  $\pi$ -backdonation. Electron density accumulation in the CN bonding region occurs without major overall charge transfer. CN-bonding is attributed to the stabilization associated with this covalent contribution and to the electrostatically favorable quadrupolar charge distribution,  $R^{+(2-\gamma)}N_{\alpha}^{-(\delta-\gamma)}N_{\beta}^{+\delta}$ , where  $\gamma \approx 0.2$  and  $\delta > 0.7$  for **1a** and **2**. This bonding model is compatible with the electron density functions of **1a** and **2**. The usual Lewis notations appear inadequate since they imply transfer of electron density from  $\text{N}_2$  to the hydrocarbon fragment and electron density depletion at  $\text{N}_{\alpha}$ .

**Automerization of Cyclopropenyldiazonium Dication.** Among the aliphatic diazonium ions the ethynyldiazonium system,<sup>14</sup> **5** is most closely related to **1** and **2** with regard to the C-hybridization of the CN-linkage. Comparative analysis of the automerizations of **1** and **5** allows to further examine these CN bonding situations. In marked contrast, the automerization of the linear ethynyldiazonium ion **5a** proceeds via an intermediate, the bridged nonclassical structure **5b**, while the automerization of **1a** is a one-step process via **1b**. The CN bond, already 0.074 Å longer in **1a** compared to **5a**, is much longer (by 0.278 Å) in the spiro-structure **1b** than in **5b**.

The major difference between these systems is that the positive charge in **1** is more delocalized. The  $\sigma$ -donation from  $\text{N}_2$  to the hydrocarbon fragment is smaller in **1a** than in **5a** ( $\rho_b(\text{CN})$ -values are 0.259 in **1a** and 0.291 in **5a**) and, because of the large positive charge of the hydrocarbon fragment in **1a**, the  $\pi$ -backdonation also is reduced. In **5a** the  $\sigma$ -donation from  $\text{N}_2$  (0.337  $e^-$ ) is entirely compensated for by effective  $\pi$ -backdonation (of

0.344  $e^-$ ) into the e-symmetric  $\pi^*$ -MOs of the diazo-function and a small net  $\text{N}_2$ -charge of  $-0.007$  results. In **1a**, the  $\pi$ -backdonation is restricted to one  $b_2$ -interaction, greatly reduced ( $N_{\pi}(\text{N}_2) = 2.049$ ), and it no longer compensates for the loss of  $\text{N}_2$ - $\sigma$ -density. A total charge of  $+0.223$  results for the diazo-function of **1a**.

$\text{N}_2$  is a potent  $\sigma_{\pi}$ -donor in **1b** and in **5b**, but only in **5b** is this density shift (over)compensated for by  $\pi$ -backdonation. Due to the electron depletion in the  $\pi$ -system of the three-membered ring  $\pi$ -backdonation becomes ineffective and, consequently, a significant charge results for the diazo-group (+0.478). Topologically both of the ring structures **1b** and **5b** are stable, but the reduced  $\pi$ -interaction in **1b** is clearly manifested in the rather concave shapes of the CN bond paths relative to the ones in **5b**.<sup>14,31a</sup>

#### Electronic Structure of 2,3-Diaminocyclopropenyldiazonium Dication

In contrast to the Mulliken analysis,<sup>12</sup> we find that the amino groups in **2** are overall electron-withdrawing. Electron density integration results in  $\text{NH}_2$ -charges of  $-0.33$  whereas the Mulliken analysis would indicate  $\text{NH}_2$ -charges of  $+0.41$  ( $\Delta = 0.74!$ ). The location of the zero-flux surface that partitions the C2N3-bonding region (Fig. 4) and the  $F_{\text{C2N3}}$ -value of 0.337 demonstrate semipolar  $\text{H}_2\text{N}-\text{C}$  bonding and we have argued above that Mulliken populations insufficiently account for such situations. Thus, the  $\text{NH}_2$ -substituents increase the electron depletion in the C-skeleton of **2** relative to **1a**. This electronic effect appears responsible for the elongation of the CC-bonds

upon H/NH<sub>2</sub>-replacement. The NH<sub>2</sub>-groups primarily affect the populations of C2 and C3; the C2-charge in **2** is higher by 0.75 compared to **1a** (+0.30).

The electron density integration and the Mulliken basis set partitioning techniques give  $\pi$ -charges that are qualitatively similar but quantitatively different (Fig. 6). Both methods—and the planarity of the NH<sub>2</sub>-groups—indicate a delocalization of NH<sub>2</sub>- $\pi$ -density that serves primarily to increase the C1-population, but the density integration technique shows that the extent of conjugative delocalization is overestimated by the Mulliken analysis, and, moreover, that this donation does not increase the  $\pi$ -populations at C2 and C3. Resonance forms with exocyclic double bonds involving the amino-nitrogens (**7B** and **7C** in reference 12) should therefore contribute little. The resonance form representing an aromatic 2e- $\pi$ -system (**7A** in reference 12) has to be assigned little importance in light of the topological analysis as well as of the Mulliken analysis. The analyses show the C1- $\pi$ -population to be higher (by 0.52 or 0.58) than the ones of the other C-atoms and such a  $\pi$ -density distribution is inconsistent with cyclic conjugation. Neither of the suggested resonance forms accounts for the N-populations of the diazo-function. Both population methods show negative (positive)  $\pi$ -charges for N1 (N2) and they indicate significant  $\pi$ -backdonation of electron density into the  $b_2$ - $\pi^*$ -MO of N<sub>2</sub>. Thus, the C2- and C3-atoms carry the major part of the  $\pi$ -charge and the  $\pi$ -donations from the NH<sub>2</sub>-groups produce a small negative C1- $\pi$ -charge.

The  $\sigma$ -populations assigned by the Mulliken method and by density integration are qualitatively different. We have pointed out above that the NH<sub>2</sub>-group ( $\sigma$ -charge = -0.59) is overall electron-withdrawing in sharp contrast to the

Mulliken data. Large  $\sigma$ -charges result for all of the C-atoms (C1 = +0.58, C2 = +0.67).

The picture that emerges for the electronic structure of **2** essentially is one in which push-pull stabilization is optimal. The diazofunction ( $\sigma$ -d,  $\pi$ -a) and the amino-groups ( $\sigma$ -a,  $\pi$ -d) synergetically enforce their bonding to the carbon-skeleton. The  $\sigma$ -depletions at C2 and C3, caused by the amino-groups, increase the C1-electrophilicity thereby optimizing the N<sub>2</sub>- $\sigma$ -donation. The concentration of  $\sigma$ -density increases the  $\pi$ -donating ability of the NH<sub>2</sub>-groups leading to a build-up of  $\pi$ -density at C1, that is,  $\pi$ -backdonation from C1 into the N<sub>2</sub>- $\pi^*$ -MO becomes more effective. This push-pull mechanism is fully consistent with the differences in the CN bonding situations in **1a** and **2** and it explains why the CN bond length is shorter in **2** than in **1a**.<sup>33</sup>

#### CN-Bond Stability and Fragment Stabilities

In a Gedanken experiment the reaction energies of the fragmentations of **1a** and **2** can be decomposed into three components, namely the energy difference  $\Delta E_1$  between the diazo-function in the diazonium ion and free N<sub>2</sub>, the energy difference  $\Delta E_2$  between the hydrocarbon fragment in the diazonium system and the free cyclopropeniumyl dication, and the energy  $\Delta E_3$  associated with the ring-opening process. The scenario is depicted schematically by the following equations, where, for example, N<sub>2</sub>(RN<sub>2</sub><sup>2+</sup>) symbolizes the diazo-function in the diazonium compound RN<sub>2</sub><sup>2+</sup>.

		1	2	
N <sub>2</sub> (RN <sub>2</sub> <sup>2+</sup> )	→ N <sub>2</sub>	$\Delta E_1$	-96.38	-38.01 (1)
R <sup>2+</sup> (RN <sub>2</sub> <sup>2+</sup> )	→ [cyc-R <sup>2+</sup> ]	$\Delta E_2$	169.14	33.10 (2)
[cyc-R <sup>2+</sup> ]	→ open-R <sup>2+</sup>	$\Delta E_3$		
RN <sub>2</sub> <sup>2+</sup>	→ [open-R <sup>2+</sup> ] + N <sub>2</sub>	$\Delta E_{\text{diss}}$	72.76	-4.91

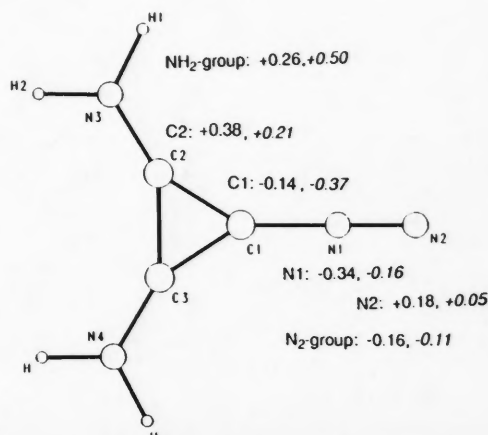
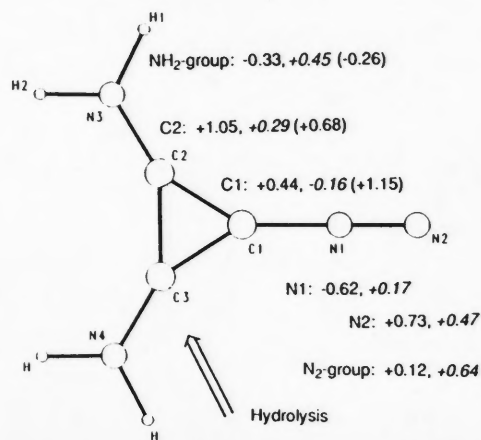


Figure 6. Comparison of Integrated Bader Populations and MNDO Mulliken Populations. The figure on the left shows total populations and  $\pi$ -charges are shown on the right. Values given in parentheses are the populations of those atoms in the dication **4**.

The energy  $\Delta E_1$  is given by the total energy of free  $N_2$  and the integrated kinetic energies within the basins of the diazo-functions since the partitioning is defined such that the virial theorem<sup>34</sup> ( $V/T = -2$  and therefore  $E = -T$ ) holds for each basin. The calculated total energies of the diazonium compounds and their fragments yield the total dissociation energies  $E_{\text{diss}}$ , and the combined reaction energies of steps (2) and (3),  $\Delta E_2 + \Delta E_3$ , can thus be determined. The reaction energy of step (1) has been evaluated with the RHF/6-31G\* wavefunctions, and therefore all energies in this discussion are at that level (and they are without VZPEs).

The dissociation of the CN bond increases the  $N_2$ -stability by  $\Delta E_1 = -96.4$  kcal/mol (1a) and  $\Delta E_2 = -38.0$  kcal/mol (2). The  $N_2$ -fragment is destabilized in the diazonium dications compared to free  $N_2$ , and it is much more destabilized in 1a than in 2. For comparison, the  $\Delta E_1$  values determined for the methyl, vinyl, and ethynyldiazonium ions are  $-39.4$ ,  $-5.6$ , and  $+44.7$  kcal/mol, respectively. The  $\Delta E_1$  values and the overall  $N_2$ -charges<sup>35</sup> are almost linearly correlated<sup>36</sup> in an inversely proportional fashion with a nonzero positive intercept as illustrated by Figure 7. The positive intercept reflects the stabilization of the neutral  $N_2$  resulting from the polarization by the electric field generated by the cation. As expected a reduction of the  $N_2$ -population decreases the  $N_2$ -stability; the slope is negative. The finding that the correlation apparently is well approximated by a linear function is more interesting considering that the  $\Delta E_1$  values reflect both the spatial characteristics of the basins and the electron density distribution therein whereas the  $N_2$ -charges reflect only the former. While the physical origins of this correlation are difficult to appreciate since many factors contribute especially to the  $\Delta E_1$

values,<sup>37</sup> the correlation apparently supports the usual assumption that the stabilities of fragments can be discussed in terms of their charges.

The increases of the stabilities of the hydrocarbon fragments associated with the formations of the diazonium ions is determined by the dissociation energies and the  $\Delta E_1$  values. The reaction energies for the combined steps (2) and (3) all are positive, that is, the hydrocarbon fragment is stabilized by association with  $N_2$  in all cases. Only in the case of ethynyldiazonium ion the union of the ethynyl cation and of  $N_2$  to form the diazonium ion stabilizes both of the fragments. The methyl- and vinyl-diazonium ions and the dication 1a are bonded because the hydrocarbon fragments are stabilized more than the diazo-functions are destabilized in the diazonium ions. And 2 exists as a local minimum only because the ring opening process is kinetically hindered.

Thus, there are two major components that cause the substantial difference in the dissociation energies of the parent diazonium dication 1a and its amino-derivative 2. While the dissociation of 1a stabilizes the  $N_2$  more than does the dissociation of 2, the former process remains endothermic because the combination of the steps (2) and (3) is about 136.0 kcal/mol more endothermic for the parent system than for its amino-derivative. With the integrated fragment stabilities (Table VI) the origin of this difference can be traced further. The C1-atoms are destabilized upon ring opening (by 0.52958 a.u. in the parent system and by 0.45634 a.u. in the derivative) because of the increase of positive charge at that position, and the C1-atom is 45.7 kcal/mol more destabilized in the parent system than in the derivative. The hydrogens or the amino-groups that are attached to C2-atoms become destabilized during the dediazonation, but not

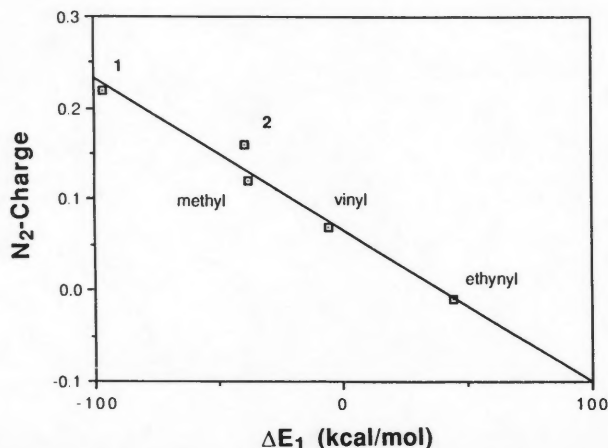


Figure 7. Correlation between the  $\Delta E_1$  values, the differences in the stabilities of  $N_2$  in the diazonium ions compared to free  $N_2$ , and the overall  $N_2$ -charges in the diazonium ions.

much. Most of the change in the CH- or CNH<sub>2</sub>-fragment stabilities, respectively, is due to the reduction of the positive charge at the C2-atoms upon formation of the dicationic 3 and 4. While each CH-group is stabilized by 0.12844 a.u., each of the CNH<sub>2</sub>-group is stabilized by 0.20137 a.u., and, thus, the two CNH<sub>2</sub>-groups in 4 are 91.5 kcal/mol more stabilized than are the two CH-groups in 3 with regard to the diazonium systems 2 and 1a, respectively. The larger destabilization of C1 (by 46.0 kcal/mol) in the parent system and the lower stabilization (by 91.5 kcal/mol) of the CH-groups with respect to the CNH<sub>2</sub>-groups add up to a value of 137.5 kcal/mol<sup>38</sup> by which the ring-opening reaction of the amino-derivative is favored over the parent system.

#### Intramolecular Polarization

We have shown that none of the resonance structures (and no combination thereof) really is compatible with the electronic structure of 2 as described by the topological properties and by the population data.<sup>39</sup> We do not conclude that the description of 2 with the resonance model should be dismissed, but instead our results suggest that a reconsideration is required of what the resonance structures actually mean in terms of electron density distribution. For this purpose the intramolecular polarizations are discussed. A firm believer in resonance theory might argue against the results of the topological electron density analysis because the integrated populations yield atom charges that are apparently too large to be compatible with other chemical models of electronic structure and reactivity.<sup>40</sup> The consideration of the molecular dipole moment shows this objection to be invalid and it introduces terms that allow for the discussion of the intramolecular polarizations.

Within the theory of atoms in molecules the molecular dipole moment is expressed as a sum of two terms,<sup>41</sup>  $\mu = \mu_c + \mu_a$ . The term  $\mu_c$ , the charge-transfer contribution, equals the sum over all atomic net charges ( $Z - N$ ) each multiplied by their respective position vector,  $\mathbf{X}$ , relative to an arbitrary origin;  $\mu_c = \sum(Z - N) \cdot \mathbf{X}$ . The second term,  $\mu_a$ , equals the sum over all basins of the first moment contributions to the molecular dipole moment that arise from the polarization of the atomic electron densities. Both of these terms are important for the description of molecular dipole moment;<sup>41</sup> that is, the large magnitude of the integrated populations are not in disagreement with the molecular dipole moment.

The first moment caused by the electron density within an atomic basin is defined as  $\mu_a' = -\int \mathbf{r}' \cdot \rho(\mathbf{r}) d\mathbf{v}$ , that is, the negative of

the integral (taken over the atomic basin) of the product between the electron density  $\rho(\mathbf{r})$  and the associated vector  $\mathbf{r}'$  that measures the distance of the position  $\mathbf{r}$  from the position of the nucleus  $Y$  ( $\mathbf{r}' = \mathbf{r} - Y$ ). The prime indicates parameters that describe atomic properties. We have determined the atomic first moments for 1a and 2 and the results are summarized in Table VII. The angles given in Table VII are those enclosed between the vector  $\mu_a'$  and the vectors defined by the atoms as indicated in the right column. With each basin partitioned by a plane normal to the direction of  $\mu_a'$  and passing through the nucleus, the direction of  $\mu_a'$  points from that part of the basin where the integral over  $\mathbf{r}' \cdot \rho(\mathbf{r})$  is positive to that part where it is negative. In other words, the direction in which atomic electron density had been polarized with regard to the nucleus is opposite to the direction of  $\mu_a'$ . We will examine the CN-linkage first and in doing so the  $\mu_a'$ -directions will become clear.

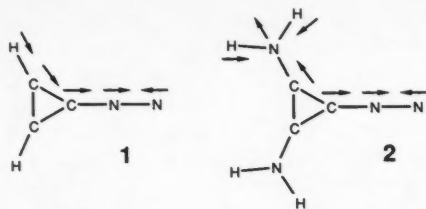
The directions of the first moments of the N1-atoms in all of the diazonium ions are directed toward the terminal N2-atoms (Table VII and

Table VII. First moments of the atoms.<sup>a</sup>

Molecule	Atom	$\mu_a$	$\mu_a$ -direction
1	C1	2.2797	0.0 C1 → N1
	N1	0.9621	0.0 N1 → N2
	N2	2.0634	0.0 N2 → N1
	C2	1.6168	13.1 C2 → C1
	H	0.2791	1.0 H6 → C2
2	C1	1.6745	0.0 C1 → N1
	N1	0.8980	0.0 N1 → N2
	N2	2.1806	0.0 N2 → N1
	C2	1.5912	148.2 C2 → C1
	N3	0.9984	179.9 N3 → C2
	H1	0.3495	0.4 H1 → N3
CH <sub>3</sub> N <sub>2</sub> <sup>+</sup>	H2	0.3490	0.4 H2 → N3
	C	1.4870	0.0 C → N1
	N1	0.7694	0.0 N1 → N2
	N2	2.0670	0.0 N2 → N1
C <sub>2</sub> H <sub>3</sub> N <sub>2</sub> <sup>+</sup>	H	0.3157	0.6 H → C
	C1	1.9991	120.4 C1 → C2
	C2	1.0129	2.4 C2 → C1
	N1	0.8749	2.0 N1 → N2
	N2	2.1798	0.0 N2 → N1
	H1	0.3121	4.1 H1 → C2
	H2	0.3101	1.8 H2 → C2
3	H3	0.3104	0.6 H3 → C1
	C2	0.7651	180.0 C2 → H
4	H	0.2555	0.0 H → C2
	C2	4.1312	0.0 C2 → N
	N	1.3929	180.0 N → C2
	H	0.3131	0.3 H → C2

<sup>a</sup> $\mu_a$  in Debye. 2.5418 D equals 1 a.u.

<sup>b</sup>See figures for numbering of atoms. Nomenclature for vinyl diazonium ion: N<sub>2</sub>-group attached to C1 via N1, H1, and H2 attached to C2, H1 is *syn* with regard to the CN-bond.

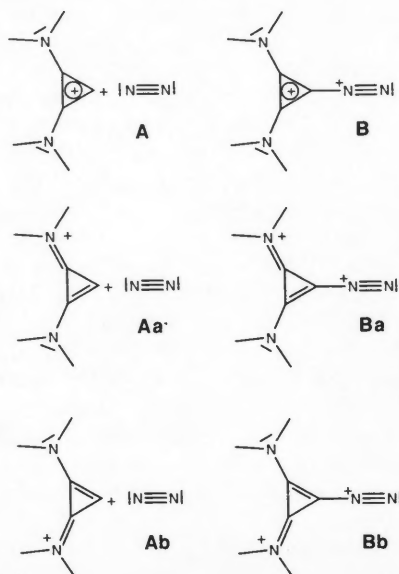


Scheme 1). While the first moments of the C1-atoms are parallel to the moments  $\mu_a'(N1)$ , the moments  $\mu_a'(N2)$  are antiparallel, e.g.  $(\rightarrow)_{C1}(\rightarrow)_{N1}(\leftarrow)_{N2}$ . The N1-atoms not only have accumulated negative charge, but their first atomic moments clearly demonstrate that the electron density within the basin of N1 is polarized toward the C1-atoms and away from the N2-atoms. In the case of the N2-atoms the electron density is polarized in such a way as to increase the electron density in the lone-pair region. While the internal polarization in the N1-basins reinforces the dipole component due to charge transfer within the  $N_2$ -group, the internal polarization of the terminal atoms reduces it. Since the first moments of the N2-atoms are more than twice as large as the  $\mu_a'(N1)$  moments, it becomes clear that the contributions of the  $N_2$ -group to the overall dipole moment are significantly smaller than the populations of the  $N_2$ -nitrogens would seem to indicate. The electron density within the C1-basins always is polarized toward the region opposite to the diazo-group. These internal polarizations are fully compatible with the CN bonding model. Partly, this compatibility reflects that both the  $\mu_a'$ -values and the topological properties on which the CN bonding model is based depend on the locations of the zero-flux surfaces. Since only the  $\mu_a'$  values include information about the location of the zero-flux surfaces and the electron density distribution within the basins, these  $\mu_a'$  values provide support for the CN bonding model that goes beyond the pure topological argument.

The  $\mu_a'$  values show an important difference in the electronic structures of 1a and amino-derivative 2. The  $\mu_a'(C2)$  moment in 1a roughly points toward the C1-atom and deviates from this direction by  $13.1^\circ$  towards the inside of the ring. This situation is typical for the association of a cationic species  $R^{n+}$  with a neutral molecule E. The center of positive charge of  $R^{n+}$  is shifted toward E as E approaches by polarization of the electron density of  $R^{n+}$  in the opposite direction. In contrast, the  $\mu_a'(C2)$  moments in 2 are directed toward the attached amino-group; the angle enclosed between  $\mu_a'(C2)$  and the  $C2 \rightarrow C1$  vector is found to be  $148.2^\circ$ . The population data show negative charges for the amino-N atoms

and the  $\mu_a'$  values of the amino-nitrogens show that the electron density within the amino-N-basins is polarized into the C-NH<sub>2</sub> bonding regions. The direction of  $\mu_a'(C2)$  shows that the direct effect of the amino-group on the polarization within the C2-basin is much more important than the secondary polarization of the C2-basin due to propagation of the C1-polarization caused by the diazo-group.

With these data on the atomic first moments the electronic structure of 2 can be reconciled with the resonance model: *Whenever a lone pair of the basic resonance structure is shifted such that a new resonance form results in which this electron pair engages in an additional (double) bond then this resonance structure should be thought of as a representation of strong polarization of the group to which the lone pair "belongs."* The example of 2 makes the point. Consider notation A in Scheme 2 as the basic Lewis structure of 2; in this structure the positive charge is located on the hydrocarbon fragment and the more electronegative groups  $N_2$  and  $NH_2$  are neutral. A represents a first approximation to the charge distribution, but it obviously suffers from the disadvantage that it does not clearly express the accumulation of electron density in the CN(N) bonding region. The more common Lewis structure B, resulting by shifting the N1-lone pair into the CN bonding region, is advantageous in this regard, but B assigns a positive charge to  $N_a$  which is incompatible with the electron density function. The notation B remains useful, nevertheless, to represent the polarization of the diazo-function *if it is kept in mind* that the polarization does not cause a full posi-



tive charge on the  $N_2$ -group as **B** would imply. The structures **Aa** and **Ab** and the structures **Ba** and **Bb**, respectively, evolve from **A** and **B**, respectively, by formal delocalization of one of the amino-N lone pairs. Again, these structures are useful to discuss the electron density distribution in **2** if the formal shift of the lone pair that leads to these notations is thought of as the direction of the internal polarization of the basin of the atom to which the lone pair belongs. The next set of formal Lewis notations would result from the forms **Aa** and **Ab** by shifting the second amino-N lone pair. However, the resulting structure with its formal CN(N) double bond and its positive (negative) charge on N1 (N2) is inconsistent with the populations and with the first moments resulting from the electronic structure analysis of **2**; such a notation would therefore be useless.

As stated in the introduction, it is stressed again that by necessity there is not one simple model that fully describes the richness of a molecular electron density distribution. Yet, we believe that the bonding model derived from the topological properties, from the populations, and from the analysis of the internal polarizations is as close to the full description of the electron density distribution as a model can be that remains simple enough to be applied routinely in discussions of electronic structure and reactivity.

## Reactivity

### *Electrophilic Sites*

The electron density analysis of the cyclopropenyldiazonium dications shows that the C2-carbon clearly is the most electrophilic site in these systems. This theoretical result, derived solely from the (observable) total electron density distribution and without recourse to MO arguments or basis set partitioning populations, explains why the hydrolysis of N-substituted derivatives of **2** proceeds via cyclopropenyldiazonium salts.<sup>12</sup>

### *Reversible Protonation*

The formation of an alkyldiazonium ion by reversible C1-protonation is probably the most remarkable reaction of these diazonium salts.<sup>12</sup> The regiochemistry of the protonation apparently is consistent with the negative Mulliken C1-charge of **2** and with frontier-orbital arguments. Mulliken populations indicate a negative C1-charge and positive  $NH_2$ -charges whereas the density integration approach to populations shows the *opposite* to be true. Both of the salts that undergo reversible protonation are *N,N*-di-

(isopropyl) derivatives of **2**, that is, the amino-groups in these systems might be slightly pyramidalized for steric reasons and the reduced push-pull stabilization would cause even lower C1- and higher  $NH_2$ -populations. We thus conclude that the site of protonation does not reflect the intrinsic properties of the electron density of **2** alone, but that *the regiochemistry of the protonation is the result of inductomeric effects.*

## CONCLUSION

Our best estimates for the reaction energies of the dediazoniations  $1 \rightarrow 3 + N_2$  and  $2 \rightarrow 4 + N_2$ , respectively, are 65.5 and  $-7.2$  kcal/mol, respectively. While **1** is thermodynamically stable with regard to this reaction channel, the loss of  $N_2$  from **2** is exothermic but kinetically hindered. Two factors have been identified that contribute to the significant difference of these reaction energies. We have found that for the diazonium dications, and for most aliphatic diazonium ions in general, the hydrocarbon fragment is *stabilized* upon CN-bond formation, whereas the diazo-group usually is *destabilized* in the process. The thermodynamic CN-bond stability with regard to dissociation depends on which of these factors dominates. While it is commonly assumed that bond formation stabilizes both of the bonded fragments, CN bonding results from stabilization of the hydrocarbon fragment only and despite the destabilization of the  $N_2$  group, that is, the cations force  $N_2$  to form diazonium ions. Specifically,  $N_2$  is stabilized 58.4 kcal/mol more in the dissociation of **1** than in the dissociation of **2**, but the former process remains endothermic because the destabilization of the cyclopropeniumyl unit during the process  $1 \rightarrow 3$  exceeds that of the corresponding process  $2 \rightarrow 4$  by more than 130 kcal/mol.

The CN linkage in the diazonium dications is qualitatively similar to the aliphatic diazonium ions. All of the topological features typical for the aliphatic diazonium ions also occur in **1** and **2**. The overall  $N_2$ -charges are more positive and the internal  $N_2$ -polarization is stronger in the dications, as expected, but the positive charge of the diazo-functions remains remarkably small. The CN-bonding model for the aliphatic diazonium ions also applies to the diazonium dications. CN-Bonding can be described with a model that involves  $\sigma$ -donation of electron density from  $N_2$  to the positively charged hydrocarbon fragment and simultaneous  $\pi$ -backdonation. Electron density accumulation in the CN bonding region occurs without major overall charge transfer. CN-Bonding is attributed to the stabilization associated with this covalent contribution and

to the electrostatically favorable quadrupolar charge distribution.

The comparative study of the diazonium dications suggests that the electronic structure of **2** may best be described by invoking a push-pull interaction between the diazo- and the amino-functions; a mechanism that synergetically enforces the bonding of both functions to the electron-depleted carbon-skeleton. This bonding model is compatible with the electron density distributions of **1a** and **2**, whereas Mulliken populations do not recover the essential features of the electronic structures. For example, in sharp contrast to Mulliken populations we find that the amino groups in **2** are overall electron-withdrawing. The integrated populations strongly suggest that the usual Lewis resonance structures are incompatible with the electronic structure of **2**. Instead of dismissing the Lewis notations entirely, a method has been proposed for the interpretation of these structures that appropriately reflects the atomic populations and their first moments. The topological description of the electronic structure can be reconciled with the resonance picture if shifts of lone pairs that result in Lewis notations with an additional (double) bond are thought of as representations of the directions of internal polarization of the atomic basins.

It is my pleasure to thank Professors Andrew Streitwieser and Kenneth B. Wiberg for providing the computational facilities for this research. This work was supported by the Fonds der Chemischen Industrie (RG), by NSF grant CHE85-02137 (ASJ) and by a grant from the Exxon Research Foundation (KBW). Two tables with the vibrational frequencies of **1a-1c** and **2-4** with descriptions of the normal modes are available from the author either by regular or electronic (CHEMRG at UMCVMB) mail.

## References

1. a. Part of this work was carried out in the Department of Chemistry, University of California, Berkeley. b. Correspondence should be directed to the author's permanent address at the University of Missouri-Columbia, Department of Chemistry, 211 Chemistry Building, Columbia, Missouri 65211.
2. Presented in part at the 195th National Meeting of the American Chemical Society, Toronto, Ontario, Canada, June 1988.
3. Review: W. Kirmse, *Angew. Chem. Int. Ed. Engl.*, **15**, 251 (1976).
4. a. K. Bott, *Chem. Ber.*, **108**, 402 (1975). b. K. Bott, *Angew. Chem. Int. Ed. Engl.*, **18**, 259 (1979) c. K. Bott, *Tetra. Lett.*, **26**, 3199 (1985).
5. H. Reimlinger, *Angew. Chem.*, **75**, 788 (1963).
6. a. D. Y. Curtin, J. A. Kampmeier, and R. J. O'Connor, *Am. Chem. Soc.*, **87**, 863 (1965). b. M. S. Newman, A. E. Weinberg, *J. Am. Chem. Soc.*, **78**, 4654 (1956). c. M. S. Newman, C. D. Beard, *J. Am. Chem. Soc.*, **92**, 7564 (1970). d. W. N. Jones, and F. W. Miller, *J. Am. Chem. Soc.*, **89**, 1960 (1967).
7. P. J. Stang, Z. Rappoport, M. Hanack, L. R. Subramanian, *Vinyl Cations*, Academic Press: New York, 1979.
8. a. R. Helwig, M. Hanack, *Chem. Ber.*, **118**, 1008, (1985). b. M. Hanack, and J. Vermehren, private communication.
9. R. Glaser, *J. Am. Chem. Soc.*, **109**, 4237 (1987).
10. M. Hanack, J. Vermehren, R. Helwig, R. Glaser, *Stud. Org. Chem. (Amsterdam)*, *Phys. Org. Chem.*, **31**, 17 (1987).
11. See also: G. Angelini, M. Hanack, J. Vermehren, and M. Speranza, *J. Am. Chem. Soc.*, **110**, 1293 (1988).
12. R. Weiss, K.-G. Wagner, C. Priesener, and J. Macheleid, *J. Am. Chem. Soc.*, **107**, 4491 (1985).
13. a. R. F. W. Bader, *Acc. Chem. Res.*, **18**, 9 (1985). b. R. F. W. Bader, T. T. Nguyen-Dang, Y. Tal, *Rep. Prog. Phys.*, **44**, 893 (1981).
14. R. J. Glaser, *J. Phys. Chem.*, **93**, 7993 (1989).
15. Quantum mechanical computations were carried out with Gaussian86 and earlier versions. *Gaussian 86*, M. J. Frisch, J. S. Binkley, H. B. Schlegel, K. Raghavachari, C. F. Melius, R. L. Martin, J. J. P. Stewart, F. W. Borowicz, C. M. Rohlfing, L. R. Kahn, D. J. Defrees, R. Seeger, R. A. Whiteside, D. J. Fox, E. M. Fleuder, and J. A. Pople, Carnegie-Mellon Quantum Chemistry Publishing Unit, Pittsburgh, PA, 1986.
16. Computations were carried out with DEC MicroVax II workstations, the DEC Vax-8600 at the Berkeley Campus Computer Facility, and on the CRAY-2 at the Pittsburgh Supercomputing Center. Electron density analysis was carried out using a MAP CSPI array processor hosted by a MicroVax II workstation.
17. a. M. M. Francl, W. J. Pietro, W. J. Hehre, M. S. Gordon, and J. A. Pople, *J. Phys. Chem.*, **77**, 3654 (1982) and references therein.
18. a. J. S. Binkley, J. A. Pople, W. J. Hehre, *J. Am. Chem. Soc.*, **102**, 939 (1980). b. M. S. Gordon, J. S. Binkley, J. A. Pople, W. J. Pietro, W. J. Hehre, *J. Am. Chem. Soc.*, **104**, 2797 (1985).
19. a. W. J. Hehre, R. Ditchfield, J. A. Pople, *J. Chem. Phys.*, **56**, 2257 (1972). b. P. C. Hariharan, J. A. Pople, *Theoret. Chim. Acta.*, **28**, 213 (1973). c. J. S. Binkley, J. S. Gordon, D. J. DeFress, J. A. Pople, *J. Chem. Phys.*, **77**, 3654 (1982). d. Six Cartesian second-order Gaussians were used for *d*-shells.
20. a. C. Møller, M. S. Plesset, *Phys. Rev.*, **46**, 1423 (1934). b. J. S. Binkley, J. A. Pople, *Int. J. Quantum Chem.*, **9**, 229 (1975). c. J. A. Pople, R. Seeger, *Int. J. Quantum Chem.*, **10**, 1 (1976). d. J. A. Pople, R. Krishnan, H. B. Schlegel, J. S. Binkley, *Int. J. Quantum Chem.*, **(14)** 91, 545 (1978). e. R. Krishnan, M. J. Frisch, and J. A. Pople, *J. Chem. Phys.*, **72**, 4244 (1980).
21. Psichk: T. J. LePage, Yale University, New Haven, Connecticut, 1988.
22. Extreme: F. W. Biegler-König, McMaster University, Hamilton, Ontario, 1980.
23. Alpha: K. Laidig, Yale University, New Haven, Connecticut, 1987.
24. Proaims: a. F. W. Biegler-König, and F. A. Duke, McMaster University, Hamilton, Ontario, 1981. b. Modifications by C. D. H. Lau, McMaster University, Hamilton, Ontario, 1983. c. Adapted for a CSPI array processor by T. J. LePage, Yale University, New Haven, Connecticut, 1987.
25. F. W. Biegler-König, R. F. W. Bader, and T.-H. Tang, *J. Comp. Chem.*, **3**, 317 (1982).

26. Compare: J. M. Bofill, J. Farras, S. Olivella, A. Sole, J. Vilarrasa, *J. Am. Chem. Soc.*, **110**, 1694 (1988).
27. Second-order perturbation theory is insufficient for the computation of these binding energies. In fact, the MP2/6-31G\*\*/RHF/6-31G\* binding energies all are worse than the RHF/6-31G\* values compared to the highest level calculations.
28. a. R. F. W. Bader, S. G. Anderson, and A. J. Duke, *J. Am. Chem. Soc.*, **101**, 1389 (1979). b. R. F. W. Bader, T. T. Nguyen-Dang, T. Tal, *J. Chem. Phys.*, **70**, 4316 (1979). c. R. F. W. Bader, *J. Chem. Phys.*, **76**, 2871 (1980). d. R. F. W. Bader, T. S. Slee, D. Cremer, E. Kraka, *J. Am. Chem. Soc.*, **105**, 5061 (1983). e. D. Cremer, E. Kraka, T. S. Slee, R. F. W. Bader, C. D. H. Lau, T. T. Nguyen-Dang, P. J. MacDougall, *J. Am. Chem. Soc.*, **105**, 5069 (1983). f. R. F. W. Bader, H. J. Essen, *J. Chem. Phys.*, **80**, 1943 (1984).
29. See for example: a. R. Breslow, *J. Am. Chem. Soc.*, **79**, 5318 (1957). b. R. Breslow, G. Ryan, *J. Am. Chem. Soc.*, **89**, 3073 (1967). c. Z. Yoshida, H. Konishi, H. Ogoshi, *Isr. J. Chem.*, **21**, 139 (1981).
30. Equivalent to the bent bond description is the MO model involving three-center bonds formed by an *sp*- and a *p*-MO of each of the C-atoms.
31. a. D. Cremer, E. Kraka, *J. Am. Chem. Soc.*, **107**, 3800 (1985). b. D. Cremer, J. Gauss, *J. Am. Chem. Soc.*, **108**, 7467 (1986).
32. For related discussions, see: a. R. Glaser, *J. Comp. Chem.*, **10**, 118 (1989). b. S. Gronert, R. Glaser, and A. Streitwieser, Jr., *J. Am. Chem. Soc.*, **111**, 3111 (1989). c. S. M. Bachrach, and A. Streitwieser, Jr., *J. Comp. Chem.*, (in press).
33. Supporting evidence is detailed in the Supplemental Material.
34. R. F. W. Bader, *The Nature of Chemical Binding, in The Force Concept in Chemistry*; B. M. Deb, Ed., Van Nostrand Reinhold Company, New York, 1981.
35. Integrated charges of the diazo-functions in methyl, vinyl, and ethynyldiazonium ions are +0.16, +0.07, and -0.01, respectively. See Ref. 14 for details.
36. The line in Figure 7 is described by  $y = -1.6677E-3 \cdot x + 6.7089E-2$  with a correlation coefficient of 0.969.
37. The polarization of the valence and of the core densities upon charge relaxation in the diazonium ions cause large and interrelated changes in the components of the energy of the topologically defined atom.
38. The small difference between this value of 137.5 kcal/mol and the value of 136.0 kcal/mol (derived from the dissociation energies and from the stabilization of the diazo-groups) is due to the numerical integrations. This small difference has no consequences for the discussion.
39. For some recent related discussion, see a. M. R. F. Siggel, A. Streitwieser, Jr., T. D. Thomas, *J. Am. Chem. Soc.*, **110**, 8022 (1988) and references therein. b. K. B. Wiberg, C. M. Breneman, K. E. Laidig, R. E. Rosenberg, *Pure & Appl. Chem.*, **61**, 635 (1989) and references therein.
40. In passing we note that one of the more frequent objection against the magnitude of the populations is that they are "intuitively" too large. "Intuition" in this regard means nothing more than "not in agreement with other, more widely used models of population analysis" and, thus, hardly provides any argument against the theory of atoms in molecules.
41. a. R. F. W. Bader, A. LaRouche, C. Gatti, M. T. Carroll, P. J. MacDougall, K. B. Wiberg, *J. Chem. Phys.*, **87**, 1142 (1987). b. T. Slee, *J. Am. Chem. Soc.*, **108**, 7541 (1986).